

13,12

Formation of Cu_6Sn_5 intermetallic in Cu/Sn thin films

© L.E. Bykova¹, S.M. Zharkov^{1,2}, V.G. Myagkov¹, Yu.Yu. Balashov¹, G.S. Patrino^{1,2}

¹Kirensky Institute of Physics, Federal Research Center KSC SB, Russian Academy of Sciences, Krasnoyarsk, Russia

²Siberian Federal University, Krasnoyarsk, Russia

E-mail: lebyk@iph.krasn.ru

Received June 9, 2021

Revised June 9, 2021

Accepted June 11, 2021

The study of the formation of the Cu_6Sn_5 intermetallic compound in Sn(55 nm)/Cu(30 nm) thin bilayer films was carried out directly in the column of a transmission electron microscope (electron diffraction mode) by heating the film sample from room temperature to 300°C and recording the electron diffraction patterns. The thin films formed as a result of a solid state reaction were monophasic and consisted of the η - Cu_6Sn_5 hexagonal phase. The temperature range for the formation of the η - Cu_6Sn_5 phase was determined. The estimate of the effective interdiffusion coefficient of the reaction suggests that the main mechanism for the formation of the Cu_6Sn_5 intermetallic is diffusion along the grain boundaries and dislocations.

Keywords: thin films, Cu_6Sn_5 intermetallic compound, transmission electron microscopy, electron diffraction.

DOI: 10.21883/PSS.2022.14.54350.139

1. Introduction

The environmental and health benefits of lead-free solders based on Cu–Sn alloys have prompted researchers to study the properties and behavior of the Cu–Sn system [1]. There is intensive formation of Cu_6Sn_5 intermetallic compound due to the reaction between Cu and Sn when soldering with Cu–Sn solders in electronic equipment [2–4]. The proportion of the intermetallic layer compared to the total thickness of the solder joint increases at the miniaturization of electronic devices. Cu_6Sn_5 intermetallic compound is also an important material in the manufacture of lithium battery anodes [5–6].

It is known that phase transformations of Cu_6Sn_5 intermetallic compound significantly affect the reliability of electronic devices. Therefore, knowledge of the crystal structure and phase transformations of the Cu_6Sn_5 intermetallic compound is required to understand adjustments in its properties during soldering and operation of electronic devices. Binary thin Sn/Cu films are a convenient object for studying structural adjustments during the production and operation of the Cu_6Sn_5 intermetallic compound.

The crystal structure of Cu_6Sn_5 has been studied and identified in several modifications by now. Differences in crystal structure are the result of adjustments in composition and depend on the processing method [7–10]. In the solid state, Cu_6Sn_5 (54.5 at.% Cu) has two crystal structures according to the phase diagram of Cu–Sn [11]. The monoclinic η' - Cu_6Sn_5 (space group $C2/c$) is stable at temperatures below 186°C, while the hexagonal η - Cu_6Sn_5 (space group $P6_3/mmc$) is stable at temperatures over 186°C. The polymorphic phase transformation $\eta \rightarrow \eta'$ occurs when the temperature drops below 186°C. According

to room temperature density data, the polymorphic transformation of $\eta \rightarrow \eta'$ Cu_6Sn_5 results in a volume expansion of 2.15% [10], which leads to undesirable internal stresses in the intermetallic layer.

This work presents the results of the synthesis of thin films of Cu_6Sn_5 intermetallic compound, carried out directly in a transmission electron microscope (TEM) column by heating a sample of a two-layer Sn/Cu film from room temperature up to 300°C (electron diffraction mode). The main parameters of the synthesis and the adjustment in the phase composition during the solid-state reaction between the Cu and Sn layers are determined.

2. Experimental techniques and sample preparation

At the preparation of Sn(55 nm)/Cu(30 nm) two-layer films, the thicknesses of Cu and Sn layers were chosen from the ratio of the composition of the Cu_6Sn_5 intermetallic compound (~ 54.5 at.% Cu, ~ 45.5 at.% Sn).

The preparation of initial two-layer Sn/Cu films included successive thermal precipitation of Cu and Sn films ~ 30 nm and ~ 55 nm thick, respectively, in vacuum at a residual pressure of $1.3 \cdot 10^{-4}$ Pa. The Cu layer was deposited on a freshly cleaved NaCl(001) single crystal heated to a temperature of 200°C, which ensured epitaxial growth of Cu(111) relative to the substrate surface. A Sn layer with a thickness of ~ 55 nm was deposited on a Cu layer at room temperature to prevent an uncontrolled reaction between the Sn and Cu layers. High-purity materials were used for evaporation: Cu (99.99%) and Sn (99.995%). The thicknesses of the Sn and Cu layers were determined

by X-ray fluorescence analysis; the total thickness of the Sn/Cu films was ~ 85 nm.

For TEM studies, the resulting Sn/Cu/NaCl(001) films were separated from the NaCl(001) substrate in distilled water at room temperature, deposited on supporting molybdenum grids for transmission electron microscopy, and placed on a heater in an electron microscope. The film sample was heated directly in the column of a transmission electron microscope using a special sample holder (Gatan Model 652 Double Tilt Heating Holder), which allows to control sample heating from room temperature to 1000°C . Samples were heated from room temperature to 300°C at a rate of $4^\circ\text{C}/\text{min}$, with electron diffraction patterns recorded after 1°C . Analysis of the electron diffraction patterns allowed to obtain data on the adjustment in the phase composition of the samples at heating.

The structure and local elemental composition of the obtained samples were studied using a JEOL JEM-2100 transmission electron microscope equipped with an Oxford Inca x-sight energy-dispersive spectrometer at an accelerating voltage of 200 kV. Analysis of the intensity of diffraction reflections on electron diffraction patterns and their interpretation were made using the Gatan Digital Micrograph software and the ICDD PDF 4+ database [12].

3. Experimental results and discussion

The initial Sn/Cu samples were two-layer thin films consisting of Sn and Cu nanolayers. The electron diffraction pattern (Fig. 1) obtained from the initial Sn/Cu film demonstrated diffraction reflections specific to the following phases: β -Sn (space group $I4_1/amd$, constants lattices: $a = 5.831 \text{ \AA}$, $b = 5.831 \text{ \AA}$, $c = 3.182 \text{ \AA}$, PDF Card № 00-004-0673) and Cu (space group $Fm-3m$, lattice constant $a = 3.615 \text{ \AA}$, PDF Card № 00-004-0836). Copper deposited on the NaCl(001) substrate had a crystal-lattice orientation [111] with respect to the substrate plane. There were no reflections from $\text{Sn}_x\text{Cu}_{1-x}$ intermetallic compounds.

The sample was heated from room temperature to 300°C at a rate of $4^\circ\text{C}/\text{min}$ in an electron microscope column (electron diffraction mode). The diffraction pattern did not change until the temperature reached 95°C , when, in addition to reflections corresponding to the Cu and β -Sn phases, diffraction reflections from the η - Cu_6Sn_5 phase appeared (space group $P6_3/mmc$, lattice constants $a = 4.206 \text{ \AA}$, $c = 5.097 \text{ \AA}$, PDF Card № 00-047-1575), which indicated the beginning of the reaction between the Cu and Sn nanolayers. Figure 2, *a, b* shows electron diffraction patterns obtained at 100°C and 200°C , which show reflections corresponding to the η - Cu_6Sn_5 phase, and the intensity of the reflections corresponding to the Cu and Sn phases decreases with increasing temperature, which indicates the overreaction between Cu and Sn. When the heating temperature became higher than the melting temperature Sn ($T_m = 231.9^\circ\text{C}$), reflections corresponding

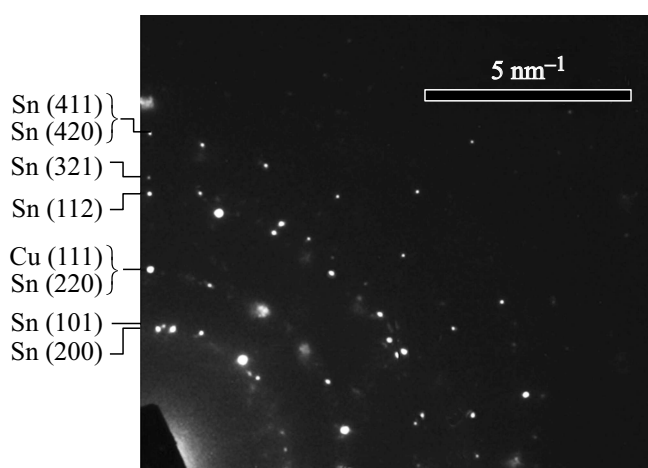


Figure 1. Electron-diffraction pattern obtained from the Sn/Cu film in the initial state.

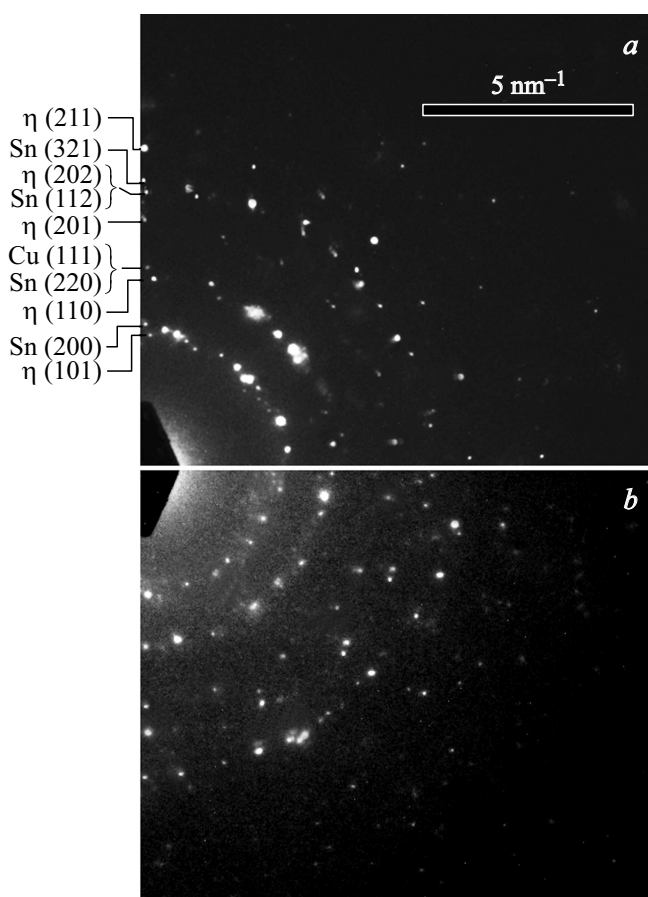


Figure 2. Electron-diffraction patterns obtained from a Sn/Cu film after heating at temperatures of 100°C (*a*) and 200°C (*b*).

to the Sn phase disappeared from the electron-diffraction pattern (Fig. 3, *a*). In the process of heating from 260°C to 300°C (Fig. 3, *a*) and after cooling the sample to 25°C (Fig. 3, *b*) there were only reflections from the hexagonal η - Cu_6Sn_5 phase in the electron-diffraction pattern, thus

confirming that Cu and Sn have completely reacted. When the film was cooled from 300 to 25°C, there was no $\eta \rightarrow \eta'$ phase transformation.

Diffraction reflections corresponding to η' -Cu₆Sn₅ phase (space group *C2/c*, lattice constant $a = 10.926 \text{ \AA}$, $b = 7.113 \text{ \AA}$, $c = 9.674 \text{ \AA}$, PDF Card № 04-014-9975) appeared on the electron-diffraction pattern after film ageing for one month at room temperature (Fig. 4). This means that a polymorphic phase transformation $\eta \rightarrow \eta'$ occurred and the film consisted of a mixture of η and η' phases.

It follows from the above that the formation of the Cu₆Sn₅ intermetallic compound occurred in the temperature range from 95–260°C, which corresponds to the reaction time $t \approx 2.5 \cdot 10^3 \text{ s}$ at a heating rate of 4°C/min. Assuming a weak temperature dependence of diffusion in the temperature range 95–260°C and using the reaction diffusion equation $d^2 = 6D_{\text{eff}} \cdot t$, the order of the effective diffusion coefficient $D_{\text{eff}} \approx 5 \cdot 10^{-16} \text{ m}^2/\text{s}$ can be evaluated, where $d = 85 \text{ nm}$ is the total film thickness. The calculated diffusion coefficient is relatively high. For most metals in thin films, the experimentally obtained diffusion coefficients are $10^{-22} - 10^{-16} \text{ m}^2/\text{s}$ at 100–800°C [13]. It can be assumed that diffusion along dislocations and grain boundaries is

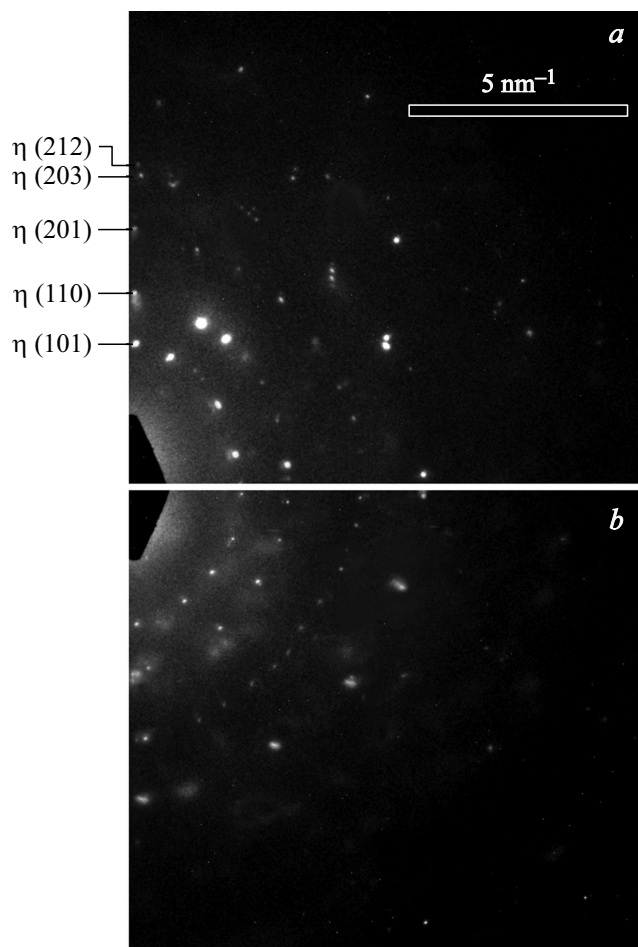


Figure 3. Electron-diffraction patterns obtained from a Sn/Cu film after heating at temperature of 300°C (a) and cooling to 25°C (b).

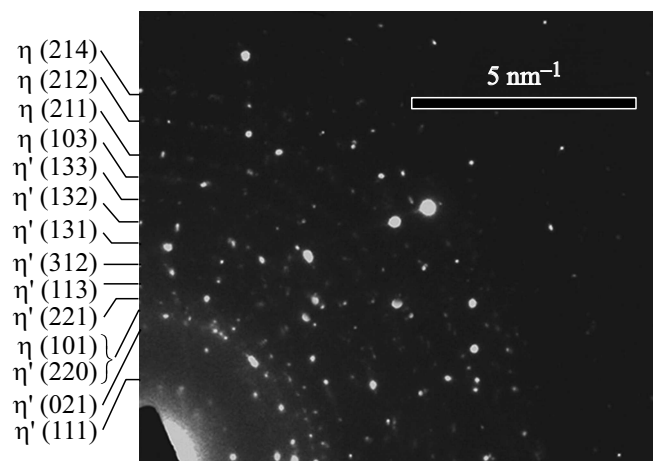


Figure 4. Electron-diffraction pattern obtained from a Cu₆Sn₅ film after holding the film for one month at room temperature.

the main mechanism that determines the formation of the Cu₆Sn₅ intermetallic compound in the solid-state reaction between Sn and Cu nanolayers.

The film image obtained by transmission electron microscopy (Fig. 5) shows the development of grain growth of the η -Cu₆Sn₅ intermetallic compound during solid-state reaction. Increasing the sample temperature from 100 to 300°C resulted in a significant growth of Cu₆Sn₅ grains (over 100 nm) (Fig. 5, b–d). The growth of grains continued as the film was cooled from 300°C to 25°C (Fig. 5, e). After film ageing for one month at room temperature, the TEM image of the film (Fig. 5, f) shows that η -Cu₆Sn₅ grains have decreased in size due to the $\eta \rightarrow \eta'$ phase transformation.

Thus, it is shown that the η -Cu₆Sn₅ phase is formed at the activation temperature $T_{\text{in}} \approx 95^\circ\text{C}$ and passes into the η' -Cu₆Sn₅ phase after film ageing at room temperature for one month. Our results are in compliance with the work by Y. Zhong [14], in which the formation of Cu₆Sn₅ nanocrystalline alloys by means of a polymorphic reversing phase transformation $\eta \leftrightarrow \eta'$, as well as with the work by Zhang [15], in which there was a phase transformation η -Cu₆Sn₅ \rightarrow η' -Cu₆Sn₅ in whiskers during ageing at room temperature for 1–40 days.

Previously, it was demonstrated that one phase is formed, which is called „the first“ and has the minimum temperature of the structural solid-state transformation in the binary system with an increase in the annealing temperature at the film interface, at first, from the set of phases present on the state diagram of a given binary system. Further, with an increase in the annealing temperature, the formation of other phases is possible with the formation of a phase sequence [16 and references are there]. In the Cu–Sn system, the structural transition $\eta \rightarrow \eta'$ in the phase diagram has a minimum temperature, so it can be concluded that in all cases, as the temperature rises at the interface between copper and tin, the Cu₆Sn₅ intermetallic compound is formed first. This is confirmed by this study and the analysis

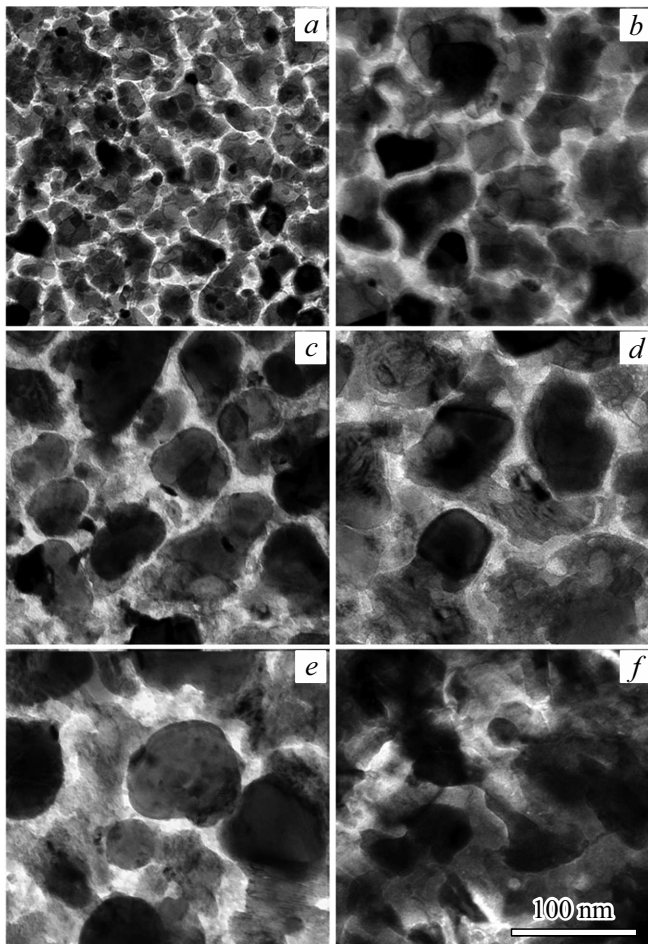


Figure 5. TEM-images obtained from the surface of the Sn/Cu film in the initial state (a) after heating at the temperature of 100°C (b), 200°C (c), 300°C (d), after cooling from 300°C to 25°C (e) and after the resulting Cu_6Sn_5 film ageing for one month at room temperature (f).

of publications by other authors studying phase formation at the Cu/Sn interface [3,10].

4. Conclusion

The Cu_6Sn_5 intermetallic compound was formed in two-layer thin films Sn(55 nm)/Cu(30 nm) by heating directly in the column of a transmission electron microscope (electron diffraction mode) from room temperature to 300°C. The thickness of the Cu and Sn layers is chosen so as to correspond to the composition ratio Cu_6Sn_5 (~ 54.5 at.% Cu, ~ 45.5 at.% Sn). The formation of the $\eta\text{-Cu}_6\text{Sn}_5$ phase begins at the activation temperature $T_{\text{in}} \approx 95^\circ\text{C}$, at a temperature of 260°C the solid-state reaction proceeds over the entire thickness of the film $d = 85$ nm. There was no phase transformation $\eta\text{-Cu}_6\text{Sn}_5 \rightarrow \eta'\text{-Cu}_6\text{Sn}_5$ during the cooling of the film in the electron microscope column from 300 to 25°C. The assessment of the effective mutual diffusion coefficient ($D_{\text{eff}} \approx 5 \cdot 10^{-16} \text{ m}^2/\text{s}$) in the course

of a solid-state reaction between Cu and Sn nanolayers allows to assume that the main mechanism for the formation of Cu_6Sn_5 intermetallic compound is diffusion along grain boundaries and dislocations. After holding the film for a month at room temperature, the hexagonal phase $\eta\text{-Cu}_6\text{Sn}_5$ partially transferred to the monoclinic phase $\eta'\text{-Cu}_6\text{Sn}_5$, which led to volumetric expansion, internal stresses and a decrease in the grain size of the Cu_6Sn_5 intermetallic compound.

Acknowledgments

The authors would like to thank V.S. Zhigalov for preparing the samples for the study.

Funding

This research was supported financially by the Russian Foundation for Basic Research (grant No. 19-43-240003). Electron microscopic studies were carried out at the Krasnoyarsk Regional Research Equipment Sharing Center of the Federal Research Center Krasnoyarsk Scientific Center of the Siberian Branch of the Russian Academy of Sciences and the Electron Microscopy Laboratory of the Research Equipment Sharing Center of the Siberian Federal University, supported under the state assignment of the Ministry of Science and Higher Education of the Russian Federation (scientific topic code FSRZ-2020-0011).

Conflict of interest

The authors declare that they have no conflict of interest.

References

- [1] S. Cheng, C.M. Huang, M. Pecht. *Microelectron Rel.* **75**, 77 (2017).
- [2] A. Kunwar, J. Hektor, S. Nomoto, Yu.A. Coutinho, N. Mocilans. *Inter. J. Mech. Sci.* **184**, 105843 (2020).
- [3] F. Somidin, H. Maeno, M.A.A. Mohd Salleh, X.Q. Trana, S.D. Mc Donalda, S. Matsumura, K. Nogita. *Mater. Character.* **138**, 113 (2018).
- [4] L. Meinshausen, H. Frémont, K. Weide-Zaage, B. Plano. *Microelectron Rel.* **53**, 1575 (2013).
- [5] R.Z. Hu, M.Q. Zeng, M. Zhu. *Electrochim. Acta.* **54**, 2843 (2009).
- [6] Ya. Xing, S. Wang, B. Fang, Y. Feng, S. Zhang. *Micropor. Mesopor. Mater.* **261**, 237 (2018).
- [7] G. Zeng, S.D. Mc Donald, J.J. Read, Q. Gu, K. Nogita. *Acta Mater.* **69**, 135 (2014).
- [8] Y.Q. Wu, J.C. Barry, T. Yamamoto, Q.F. Gu, S.D. Mc Donald, S. Matsumura, H. Huang, K. Nogita. *Acta Mater.* **60**, 6581 (2012).
- [9] D.K. Mu, S.D. Mc Donald, J. Read, H. Huang, K. Nogita. *Solid State Mater. Sci.* **20**, 55 (2016).
- [10] M.Y. Li, Z.H. Zhang, J.M. Kim. *Appl. Phys. Lett.* **98**, 201901 (2011).
- [11] N. Saunders, A.P. Miodownik. *Bull. Alloy Phase Diagr.* **11**, 278 (1990).

- [12] Powder Diffraction File (PDF 4+, 2018), Inorganic Phases Database, International Center for Diffraction Data (ICDD), Swarthmore, PA, USA.
(<http://www.icdd.com/products/pdf4.htm>)
- [13] A. Makovec, G. Erdélyi, D.L. Beke. *Thin Solid Films*, **520**, 2362 (2012).
- [14] Y. Zhong, C. Wang, J. Wang, H. Ma, S. Krishnamoorthy, V. Paley, Z. Weng, S. Jin. *Mater. Res. Lett.* **8**, 431 (2020).
- [15] Z.H. Zhang, C.W. Wei, J.J. Han, H.J. Cao, H.T. Chen, M.Y. Li. *Acta Mater.* **183**, 340 (2020).
- [16] V.G. Myagkov, L.E. Bykova, V.S. Zhigalov, A.A. Matsynin, D.A. Velikanov, G.N. Bondarenko. *J. Alloys Compd.* **861**, 157938 (2021).